JOURNAL OF VIROLOGY, Aug. 2004, p. 7916–7924 Vol. 78, No. 15
0022-538X/04/$08.00+0 DOI: 10.1128/JVI.78.15.7916–7924.2004

A Mouse-Adapted Enterovirus 71 Strain Causes Neurological Disease in Mice after Oral Infection

Ya-Fang Wang,[1] Chun-Ting Chou,[2] Huan-Yao Lei,[2] Ching-Chuan Liu,[3] Shih-Min Wang,[3] Jing-Jou Yan,[4] Ih-Jen Su,[5] Jen-Reng Wang,[6] Trai-Ming Yeh,[6] Shun-Hua Chen,[2] and Chun-Keung Yu[2]*

Institute of Basic Medical Sciences[1] and Departments of Microbiology and Immunology,[2] Pediatrics,[3] Pathology,[4] Clinical Medicine,[5] and Medical Technology,[6] College of Medicine, National Cheng Kung University, Tainan, Taiwan, Republic of China

Received 16 January 2004/Accepted 19 April 2004

A mouse-adapted enterovirus 71 (EV71) strain with increased virulence in mice, MP4, was generated after four serial passages of the parental EV71 strain 4643 in mice. Strain MP4 exhibited a larger plaque size, grew more rapidly, and was more cytotoxic in vitro than strain 4643. Although strains 4643 and MP4 both induced apoptosis of SK-N-SH human neuroblastoma cells, MP4 was more virulent than 4643 in 1-day-old mice (50% lethal doses, 10^2 and 10^4 PFU/mouse, respectively). Strain MP4 (5×10^6 PFU/mouse), but not 4643, could orally infect 7-day-old mice, resulting in rear-limb paralysis followed by death 5 to 9 days after inoculation with the virus. Histopathologically, neuronal loss and apoptosis were evident in the spinal cords as well as the brain stems of the infected mice. The limb muscles displayed massive necrosis. There was early and transient virus replication in the intestines, whereas the spinal cord, brain, and muscle became the sites of viral replication during the late phase of the infection. Virus transmission occurred among infected and noninfected cagemates, as demonstrated by the occurrence of seroconversion and the presence of viable viruses in the stool samples of the latter. Protection against EV71 challenge was demonstrated following administration of hyperimmune serum 1 day after inoculation with the virus. Nucleotide sequence analysis of the genome of EV71 strain MP4 revealed four nucleotide changes on the 5′ untranslated region, three on the VP2 region, and eight on the 2C region, resulting in one and four amino acid substitutions in the VP2 and 2C proteins, respectively.

Enterovirus 71 (EV71), a neurotropic virus with undefined pathogenesis, has caused significant morbidity and mortality worldwide and especially in the Asia-Pacific region since it was first described in 1969 in the United States (1, 2). EV71 infections are generally mild, such as hand-foot-and-mouth disease (HFMD) and herpangina, but occasionally lead to severe diseases such as aseptic meningitis, poliomyelitis-like paralysis, and possibly fatal encephalitis in neonates. The outbreak of EV71 in Taiwan in 1998 killed 78 children, and since then EV71 infection has become endemic in Taiwan (8, 16). Brain stem encephalitis associated with pulmonary edema and cardiac insufficiency were the primary manifestations in patients with neurologic involvement (10, 16, 28). The predominant pathological findings were in the thalamus, pons, midbrain, medulla oblongata, and spinal cord, with intense neutrophil and mononuclear cell infiltrates. There was severe congestion with focal hemorrhage and edema in the lungs (21). Although EV71 was recovered from the mycocardium, there was only mild degeneration of the mycocardium. Neurogenic shock as a result of brain stem encephalitis has been proposed as the cause of pulmonary and cardiac complications (13, 16). It has also been postulated that overwhelming virus replication combined with damage in tissues with the induction of toxic inflammatory cytokines is one possible pathogenesis (14, 15, 27). Alteration of the cellular immunity of the host has also been suggested to be related to the severity of the disease (30).

Previous studies of the molecular epidemiology of EV71 were unable to identify neurovirulence determinants (18, 29). Zheng et al. (32) demonstrated that the 5′ untranslated regions (UTRs) of EV71 isolates from HFMD patients were different from those from patients with aseptic meningitis. The 5′ UTR contains the internal ribosome entry site (IRES) that regulates enterovirus replication (17). Specific nucleotide mutations within the IRES are known to seriously impair or eliminate the virulence phenotypes of polioviruses (6, 19, 22) and coxsackieviruses B1 (24) and B3 (5, 26). There has been no progress in the research on the pathogenesis of EV71 because suitable animal models have not been established. Experimental infections with EV71 in neonatal mice (4, 31) and monkeys (7) have been reported. It was recently demonstrated that EV71 could infect 1-day-old mice via oral inoculation (3). In that study it was reported that a mouse-adapted EV71 strain, MP4, which contains point mutations in the VP2 and 2C regions and the 5′ UTR, caused a fatal disease in 7-day-old mice with poliomyelitis and myelitis after oral inoculation. Neutralizing antibody (Ab) readily attenuated the disease in EV71-infected mice. The similarity of this oral infection model to the human EV71 disease suggests that it is a unique tool for studying EV71 pathogenesis and vaccine development.

* Corresponding author. Mailing address: Department of Microbiology and Immunology, College of Medicine, National Cheng Kung University, Tainan, Taiwan, Republic of China. Phone: 886-6-2353535, ext. 5673. Fax: 886-6-2082705. E-mail: dckyu@mail.ncku.edu.tw.

MATERIALS AND METHODS

Cells and viruses. RD (rhabdomyosarcoma), Caco-2 (human colorectal carcinoma), and SK-N-SH (human neuroblastoma) cells (American Type Culture Collection, Manassas, Va.) were maintained in Dulbecco's modified Eagle's

medium containing 20 or 10% fetal bovine serum (for Caco-2 cells or other cell lines, respectively) plus 2 mM L-glutamine, 100 IU of penicillin, and 100 μg of streptomycin per ml. EV71/Tainan/4643/98 stock virus (GenBank accession number AF304458) (29) was grown in RD cells. For preparation of mouse-adapted EV71 strains, the parental EV71 strain 4643 was intraperitoneally (i.p.) inoculated into 1-day-old ICR mice (Laboratory Animal Center, National Cheng Kung University Medical College, Tainan, Taiwan). Virus was isolated from the brain tissues of infected animals by one passage in RD cells. The viral strain derived from the fourth passage in mice was used and designated MP4. The MP4 strain shows positive reactivity to anti-EV71 monoclonal antibody (MAb) (Chemicon, Temecula, Calif.) with indirect immunofluorescence staining of infected RD cell cultures and to murine hyperimmune sera with Western blotting (data not shown). To prepare virus stocks, viruses were propagated for one more passage in RD cells. Working stocks contained 10^8 PFU per ml.

One-step growth kinetics and cytotoxicity of EV71. RD, Caco-2, and SK-N-SH cell monolayers in 24-well plates (10^6 cells) were infected with the parental strain 4643 or the mouse-adapted strain MP4 at a multiplicity of infection (MOI) of 1 or 10 for 1 h at 35°C. The cells were washed and then cultivated in Dulbecco's modified Eagle's medium containing 2% fetal bovine serum. Virus titers were determined at different intervals by a plaque assay using RD cell monolayers in 24-well plates (9). For comparing the cytotoxicities of EV71 strains, SK-N-SH cells (2×10^4) were seeded in 96-well plates for 18 h before infection with either 4643 or MP4 at the same dose (eight wells). Cell viability was monitored at different intervals by a colorimetric assay (Cell Counting Kit-8; Dojindo Molecular Technologies, Gaithersburg, Md.).

Detection of apoptosis. Caco-2 and SK-N-SH monolayers were infected with strain 4643 or MP4 at an MOI of 1 as described above. Infected cells were harvested at different intervals, and the whole-cell lysates were prepared for Western blot analysis with anti-caspase 9 MAb (clone 96-2-22; Upstate Biotechnology Inc., Lake Placid, N.Y.) for detection of both the proform and the cleavage form of caspase 9. Protein bands were visualized with chemiluminescent reagent (Western Lightning; Perkin-Elmer, Boston, Mass.). In other experiments, EV71-infected cells were stained with phycoerythrin-conjugated Annexin V (BD Pharmingen, San Diego, Calif.) and examined by flow cytometry (BD Immunocytometry Systems, San Jose, Calif.).

Virus inoculation of mice. To determine the 50% lethal dose (LD_{50}), specific-pathogen-free, 1-day-old ICR mice ($n = 5$ or 6) were inoculated i.p. with 100 μl of serially diluted EV71 (from 10^{-1} to 10^{-7}). The survival of the mice was monitored daily, and the LD_{50} was calculated as described by Reed and Muench (23a). For oral infection experiments, a 24-gauge feeding tube was used to inoculate 10 to 12 7-day-old ICR mice per os (p.o.) with the virus (200 to 300 μl) after 8 h of fasting. The control mice were given RD cell lysate and kept either in the same cage with the infected mice or in a separate cage. The animals were observed daily for clinical signs, weight gain or loss, and mortality and were killed at various times postinoculation. Generally, mice were killed when signs of clinical illness were evident. For protection studies, heat-treated (56°C, 30 min) pooled sera of EV71-infected adult mice with a neutralizing titer (NT) of 1:128 (31) were injected i.p into the orally infected mice 1 day postinoculation (dpi). The control animals were given sera from naïve mice. The institutional animal care and use committee approved all animal protocols.

Histopathology and TUNEL assay to detect apoptotic cells in CNS. For each experimental group, half of the animals (five or six mice) were subjected to histopathologic examination, while the other half were subjected to virus detection assays. After euthanasia, the cervical, thoracic, and abdominal cavities of the mice were opened, and the mouse tissues were fixed by immersion in 10% buffered formalin for 48 h. The tissues were bisected, embedded in paraffin, and stained with hematoxylin and eosin or Nissl stain (central nervous system [CNS] samples only). The number of neural cell bodies that were Nissl stain positive in the ventral horn regions were counted in each of two duplicate slides (magnification, ×400). In other experiments, the brain and spinal cord en bloc were removed from each mouse after perfusion with ice-cold phosphate-buffered saline, fixed in formaldehyde, and embedded in paraffin. Apoptotic cells in tissue sections (8 μm thick) were visualized using a terminal transferase-mediated dUTP nick-end labeling (TUNEL) kit (ApoAlert DNA fragmentation assay kit; Clontech, Palo Alto, Calif.) according to the manufacturer's instructions. Apoptotic cells were examined with a fluorescent microscope.

Viral titers in tissues. Blood samples were collected after axilla dissection and stored at −70°C. After perfusion with isotonic saline containing EDTA, tissue samples were aseptically removed, weighed, and stored at −70°C. The tissue samples were homogenized in sterile phosphate-buffered saline (10%, wt/vol), disrupted by three freeze-thaw cycles, and centrifuged. Virus titers in clarified supernatants and blood were determined by plaque assays as described above and expressed as log PFU per milligram of tissue or per milliliter of blood. The lower limit of virus detection was 20 PFU. For determination of viral titers in stools, we assayed the distal portion of the colon (with stools) at 1 and 7 dpi and stool samples from individual mice collected on sterile gauze at 14 dpi.

Immunohistochemical staining. Perfused tissues were immediately frozen in a liquid nitrogen-cold hexane bath in 100% OCT compound (Miles, Elkhart, Ind.). Cryosections (8 to 10 μm thick) (CM1800; Leica, Wetzlar, Germany) were mounted on poly-L-lysine-coated slides, air dried, and fixed in 3.7% paraformaldehyde for 10 min and then in cold acetone for 3 min. The sections were incubated with 0.3% H_2O_2 for 10 min and then with MOM reagent (Vector Laboratories, Burlingame, Calif.) for 1 h. The sections were incubated with anti-EV71 MAb (1:5,000 dilution; Chemicon) overnight at 4°C, followed by peroxidase-conjugated secondary Ab (1:7,500 dilution) for 1 h at room temperature. The sections were developed with aminoethyl carbazole (AEC substrate kit; Zymed, San Francisco, Calif.) and examined with a light microscope after counterstaining with hematoxylin. Control sections were incubated with medium instead of MAb.

Flow cytometric analysis. The spleens were removed from the mice after euthanasia and mechanically disrupted. Red blood cells were removed into a lysing solution containing 20 mM NH_4Cl, 10 mM $KHCO_3$, and 0.1 mM EDTA. After washing, a single-cell suspension (10^6 cells in 1 ml of Hanks balanced salt solution containing 2% fetal calf serum and 0.1% sodium azide) was incubated with anti-CD16/CD32 MAb (Fc blocker; 2.4G2) followed by fluorescein isothiocyanate-conjugated anti-CD3e (145-2C11) or CD4 (H129.19) and phosphatidylethanolamine-conjugated anti-CD8a (53-6.7) or B220 (RA3-6B2) MAbs (BD Pharmingen) for 30 min on ice. After the stained cells were washed, they were quantified by flow cytometry as described above. Isotype-matched MAb-stained cells were used as a background control in all experiments.

5′ UTR sequence. The 5′ end of the viral RNA of three EV71 clinical isolates, 4643, 6356, and 5746 (GenBank accession number AF304457), and the mouse-adapted strain MP4 were amplified for sequence analysis by using the GibcoBRL system for 5′ rapid amplification of cDNA ends (Life Technologies, Gaithersburg, Md.) as described previously (29). Briefly, a specific primer (5′-GTAGC GTTTCCATCAAACT-3′, nucleotides [nt] 1903 to 1921) was used to transcribe the 5′ ends of viral RNAs into cDNA. A homopolymeric tail was then added to the 3′ end of the cDNA with terminal deoxynucleotidyltransferase (GibcoBRL) and dCTP. The tailed cDNA was amplified by PCR with an anchor primer for 5′ rapid amplification of cDNA ends and a primer for strain 4643 (5′-TGTCCCA ATGACATACTCT-3′, nt 1335 to 1353).

Whole-genome sequence. The full-length nucleotide sequences of EV71 strains 4643 and MP4 were determined as previously described (29). In brief, viral RNA was converted to cDNA with an oligo(dT) primer and reverse transcriptase. Nucleotide comparisons were performed with the GAP program of the Genetics Computer Group sequence analysis package (University of Wisconsin). Multiple sequence alignments were generated using the PILEUP program of the Genetics Computer Group. The secondary structure was predicted using the GOR IV program (IBCP, Lyons, France).

Statistics. The plaque sizes, one-step growth curves, cell viabilities, and apoptosis values were analyzed by the Mann-Whitney U test, and survival rates were analyzed by log-rank analysis. The results are expressed as means ± standard errors of the means (SEM). A P value of <0.05 was considered to be significant.

RESULTS

Increased virulence of mouse-adapted EV71 in vitro and in vivo. After serial passages, the mouse-adapted EV71 strain MP4 was generated. Strain MP4 was different in vitro from the parental strain, 4643, with respect to its larger plaque size in RD cells (4643 versus MP4, 0.21 ± 0.02 cm versus 0.41 ± 0.04 cm; $P < 0.05$) and its growth rate (Fig. 1A). A one-step growth curve showed that strain MP4 grew more rapidly than strain 4643 in RD, SK-N-SH, and Caco-2 cells. The titers of MP4 were approximately 1-log-fold higher than those of 4643 in these cells. Furthermore, strain MP4 was more cytotoxic to SK-N-SH cells than was strain 4643 (Fig. 1B). Both 4643 and MP4 induced the cleavage form of caspase 9 of SK-N-SH cells after incubation for 12 h, which, however, was not detected in Caco-2 cells until after 24 h (Fig. 2A). Annexin V staining confirmed that EV71 induced apoptosis of SK-N-SH cells (>30% at 12 h and >50% at 24 h), which was found to occur

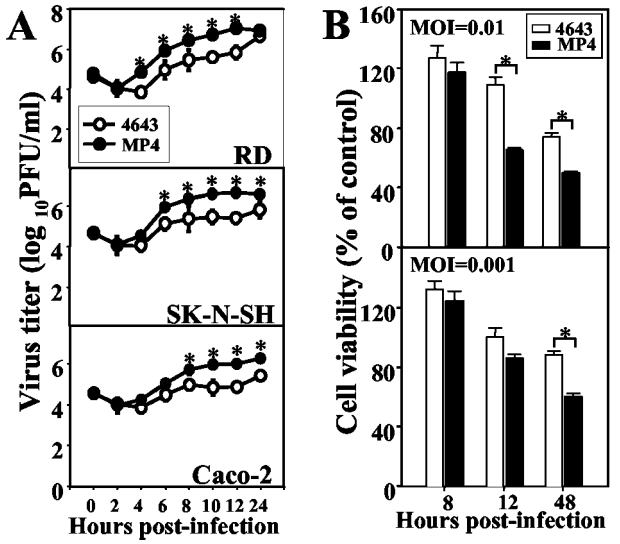

FIG. 1. Mouse-adapted EV71 grows more rapidly and is more cytotoxic than the parental strain. (A) One-step growth curves of the parental EV71 strain Tainan/4643/98 and the mouse-adapted strain MP4 in RD, SK-N-SH, and Caco-2 cells were determined as described in Materials and Methods. (B) SK-N-SH cells (2×10^4) grown in 96-well plates were infected with 4643 or MP4, and cell viability was determined at the times indicated. Data represent the means ± SEM of results of three independent experiments performed in triplicate (A) and of two experiments with eight duplicates (B). *, $P < 0.05$.

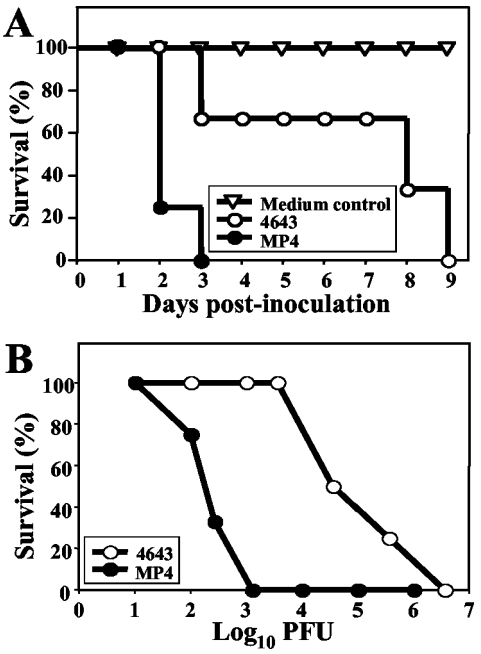

FIG. 3. The mouse-adapted EV71 strain is more virulent than the parental strain in 1-day-old mice. One-day-old ICR mice were inoculated i.p. with the parental (Tainan/4643/98) or mouse-adapted (MP4) EV71 strain at 3×10^6 PFU/mouse (A) or 10^1 to 10^7 PFU/mouse (B). Survival was then monitored daily after infection. Control mice were given cell lysate instead of virus suspension. Each group contained six to eight mice.

more rapidly and extensively than that of Caco-2 cells (20 to 25% at 48 h) (Fig. 2B). Furthermore, apoptosis was more robust in MP4-infected SK-N-SH cells than in 4643-infected SK-N-SH cells ($P < 0.05$). Since it was previously demonstrated that i.p. inoculation with strain 4643 caused significant mortality in 1-day-old mice (31), we therefore compared the in vivo virulence levels of MP4 and 4643. MP4 infection (3.0×10^6 PFU, i.p.) of 1-day-old mice resulted in death within 2 to 3 days with an average survival time of 1.3 days, while the same dose of 4643 killed the animals within 8 to 9 dpi (average survival time, 5.7 days) (Fig. 3A). The calculated LD_{50} of MP4 was 4.2×10^2 PFU per mouse, and the LD_{50} of 4643 was 5.0×10^4 PFU per mouse (Fig. 3B). These findings indicate that MP4 exhibited greater virulence than 4643 and was highly pathogenic for mice.

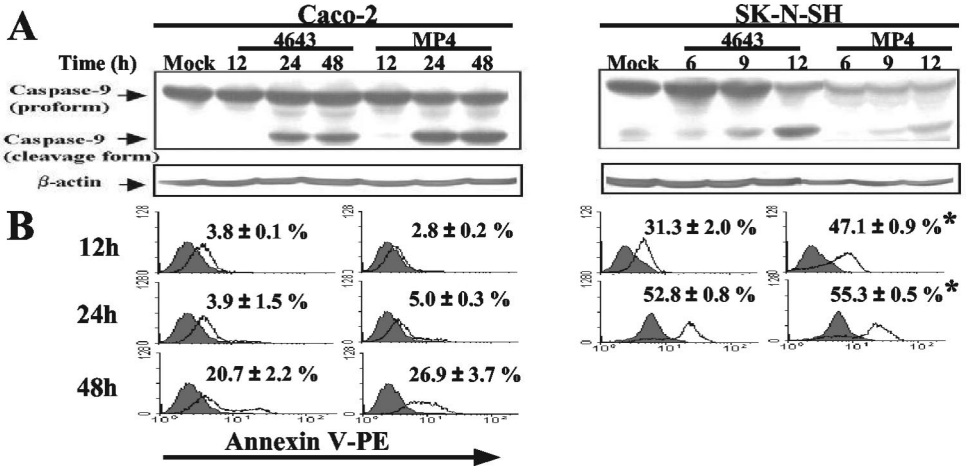

FIG. 2. EV71 induces apoptosis of Caco-2 and SK-N-SH cells. (A) Caco-2 or SK-N-SH cells were infected with the parental (Tainan/4643/98) or mouse-adapted (MP4) EV71 strain at an MOI of 1. The expressions of both the proform and the cleavage form of caspase 9 in whole-cell lysates were determined by Western blotting. (B) Apoptosis of EV71-infected cells was determined by flow cytometry after staining with Annexin V. Values are the means ± SEM of results of three independent experiments. *, P value of <0.05 compared with the results for the same cell type infected with 4643.

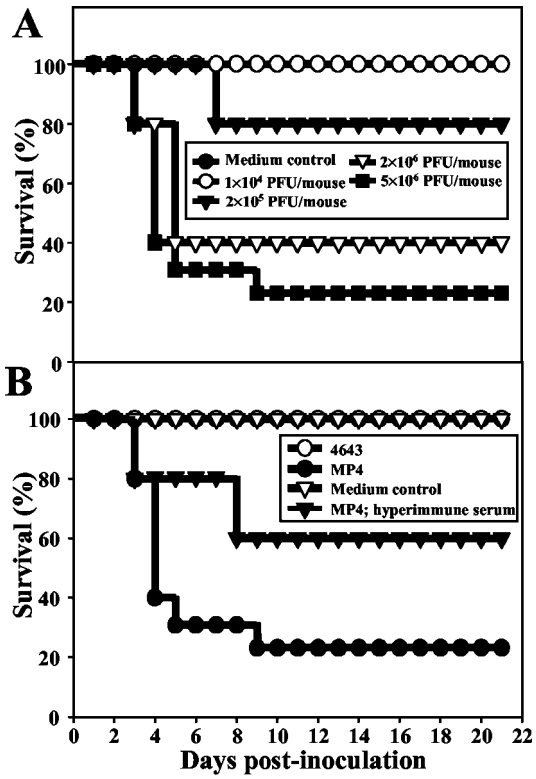

FIG. 4. Mouse-adapted EV71 induces death in mice after oral inoculation. Seven-day-old ICR mice were orally inoculated with the parental (Tainan/4643/98) or mouse-adapted (MP4) EV71 strain at 1×10^4 to 5×10^6 PFU/mouse (A) or 5×10^6 PFU/mouse (B), both at 200 μl, with or without i.p. administration of mouse anti-EV71 serum (50 μl). Survival was then monitored daily after infection. Control mice were given cell lysate instead of virus suspension. Each group contained six to eight mice.

Oral inoculation of mouse-adapted EV71 results in mortality which can be prevented by neutralizing Ab. EV71 is an enteric virus, and to understand its pathogenesis, the disease should be evaluated after oral infection. In an attempt to develop an EV71 oral infection model, we intragastrically inoculated either 4643 or MP4 into 7-day-old mice. We demonstrated that oral inoculation of MP4 resulted in a dose-dependent mortality. Approximately 70 to 80% of the animals died at 7 to 8 dpi with a challenge dose of 5×10^6 PFU/mouse (Fig. 4A). The mice consistently displayed weakness, weight loss, and rear-limb paralysis before death. The survivors either appeared normal or exhibited weakness and a failure to gain weight. The dams and the mock-infected littermates showed no sign of illness and remained healthy throughout the 21-day observation period. However, they developed anti-EV71 Ab, and viable viruses were present in the stool samples (Table 1), indicating that transmission by the oral-fecal route occurs. Postinfection treatment (at 1 dpi) with pooled hyperimmune sera from infected adult mice (NT, 1:128) increased the survival rate to 60% (Fig. 4B). In contrast to MP4, 4643 caused neither disease nor mortality when it was acquired via p.o. inoculation (Fig. 4B).

Histopathologic changes in mice infected with mouse-adapted EV71. In agreement with the neurological symptoms, neuronal degeneration and loss, neuronophagia, and vessel congestion accompanying a mild neutrophilic infiltration were consistently observed in the spinal cords, particularly in the ventral horn areas, of MP4-infected mice before death (6 dpi) (Fig. 5). Nissl staining revealed that there was a 20 to 30% decrease in the number of neuronal bodies in these areas compared to the number in the same areas in mock-infected mice (Fig. 6). The numbers of cells staining Nissl positive in the control and infected mice were 190 ± 16 and 149 ± 7 in the cervical section, 216 ± 24 and 155 ± 54 in the thoracic section, and 178 ± 26 and 142 ± 17 in the lumbar section, respectively (five to six mice per group; all P values were <0.05). Numerous TUNEL-positive neurons could be seen in the brains and spinal cords (Fig. 6). The white matter was spongelike in the tissue close to the damaged gray matter but generally unaffected. A mild degree of gliosis with vascular dilution and congestion was occasionally seen within the gray matter of the brain stem. No lesions were observed in the cerebral cortex and basal ganglia. The limb muscles revealed massive and widespread necrotizing myositis with few inflammatory infiltrates (Fig. 5). There was a generalized decrease in the amount

TABLE 1. Transmission of EV71 among littermates[a]

Group	Day after infection	Serum anti-EV71 titer (OD_{450} ± SEM[b])	Serum NT titer	Stool viral titer (log PFU/mg ± SEM)[b]
Naïve mice (7 days old)		0.126 ± 0.017	0	0
EV71-infected mice	1	0.126 ± 0.007	0	3.3 ± 0.1*
	7	0.529 ± 0.030*	32 ± 16*	0.2 ± 0.1*
	14	0.516 ± 0.006*	ND	0
Mock-infected littermates	1	0.128 ± 0.007	0	0.3 ± 0.1*
	7	0.248 ± 0.025*	0	0
	14	0.179 ± 0.013*	ND	0
Dams of EV71-infected mice	7	0.370 ± 0.002*	0	0
	14	0.285 ± 0.001*	ND	ND

[a] Seven-day-old ICR mice ($n = 6$) were orally inoculated with EV71 strain MP4 (5×10^6 PFU/mouse; 200 μl). Mock-infected littermates ($n = 6$) were given medium and reared by the same dam. *, P value of <0.05 compared with results for naïve mice. OD_{450}, optical density at 450 nm. ND, not determined.

[b] For stool viral titration, distal colon tissue was used at 1 and 7 dpi, and stool samples were used at 14 dpi.

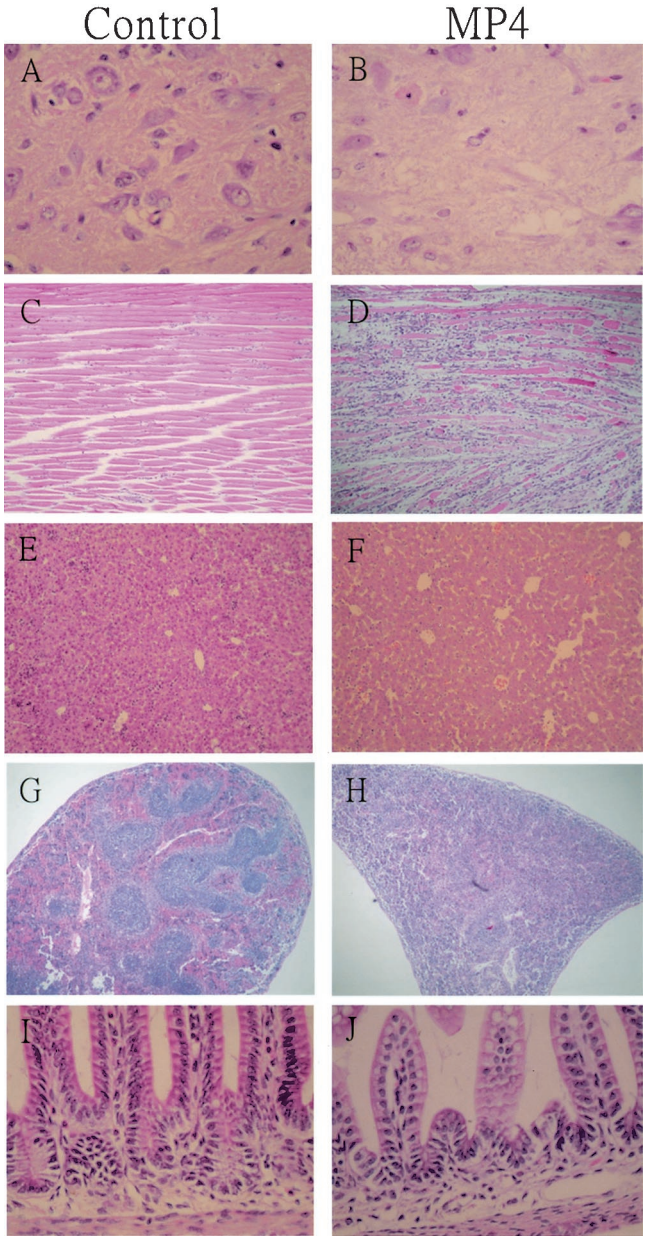

FIG. 5. Representative histology of various tissues of EV71-infected mice. Seven-day-old ICR mice were orally inoculated with cell lysate (mock control) or the mouse-adapted EV71 strain (MP4) (5×10^6 PFU/mouse), and tissues were examined histopathologically at 6 dpi as described in Materials and Methods. Typical lesions seen in MP4-infected mice include neuronal loss in ventral horns of the spinal cord (A and B), severe necrotizing myositis (C and D), decreased hematopoiesis in the liver (E and F), splenic atrophy (G and H), and villous blunting in the small intestine (I and J; 1 dpi). Hematoxylin and eosin stain. Magnifications, ×400 (A, B, I, and J), ×100 (C to F), and ×40 (G and H).

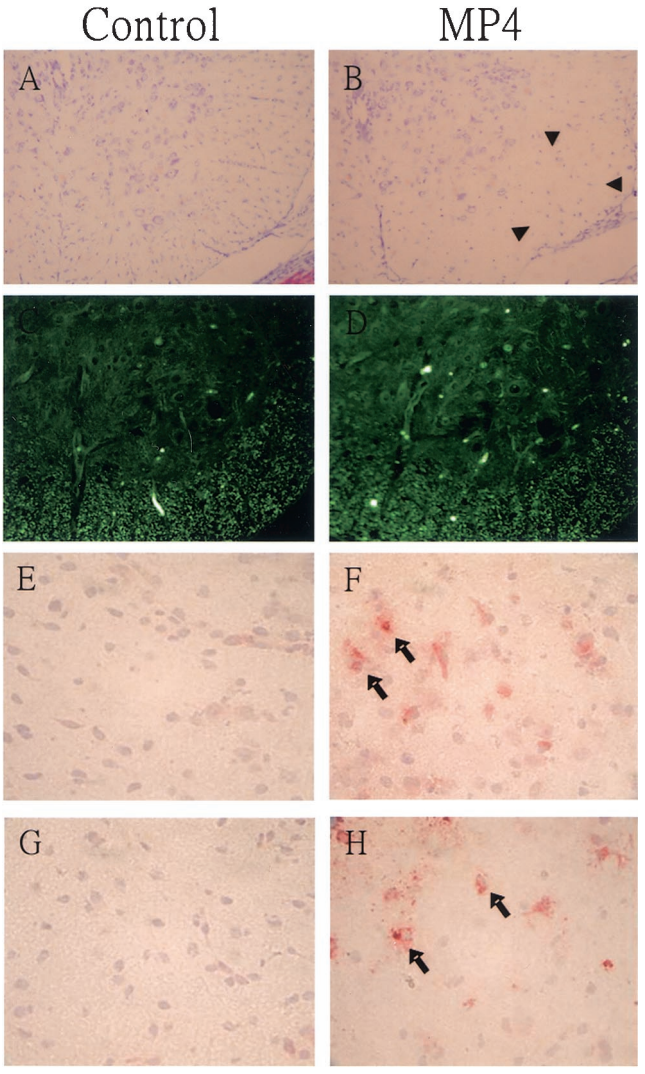

FIG. 6. Neuronal loss, apoptosis, and VP-1 expression in EV71-infected neural tissues. Seven-day-old mice were orally inoculated with cell lysate (mock control) or the mouse-adapted EV71 strain (MP4) as described in the legend to Fig. 5. Representative sections are shown, demonstrating neuronal loss (indicated by arrowheads) and apoptosis as detected in the ventral horns of the thoracic spinal cord by Nissl staining (A and B) and TUNEL (C and D), respectively, following inoculation with EV71. The immunohistochemical expression and localization of VP-1 (indicated by arrows) are shown for tissues from the brains (E and F) and spinal cords (G and H) of control and MP4-infected mice. Magnifications, ×100 (A to D) and ×400 (E to H).

of hematopoietic tissues in the liver. Lymphoid organs, including the spleen and thymus, were greatly atrophied, with severe myeloid and lymphoid depletion but no necrosis (total number of splenocytes for control versus infected mice, $7.7 \times 10^6 \pm 1.3 \times 10^6$/ml versus $2.2 \times 10^6 \pm 1.2 \times 10^6$/ml; three mice per group; $P < 0.05$). Concomitantly, flow cytometry revealed that the percentage of lymphocyte subpopulations in the spleen was significantly decreased in infected mice at 6 dpi (CD3, 25.1% ± 5.3% versus 7.6% ± 0.6%; CD4, 18.5% ± 4.7% versus 6.8% ± 0.2%; CD8, 5.6% ± 1.3% versus 1.4% ± 0.8%; B220, 55.4% ± 7.3% versus 26.9% ± 3.4% [for control versus infected mice]; three mice per group; all P values were <0.05). No obvious abnormalities were seen in the hearts and lungs. In the early stage of infection (i.e., 1 dpi), villous blunting and crypt hyperplasia were prominent in the small intestines (Fig. 5). Strain 4643-infected mice did not show any abnormality in any of the tissues examined, except that the intestines displayed a change similar to that observed in the intestines of the MP4-infected mice (data not shown).

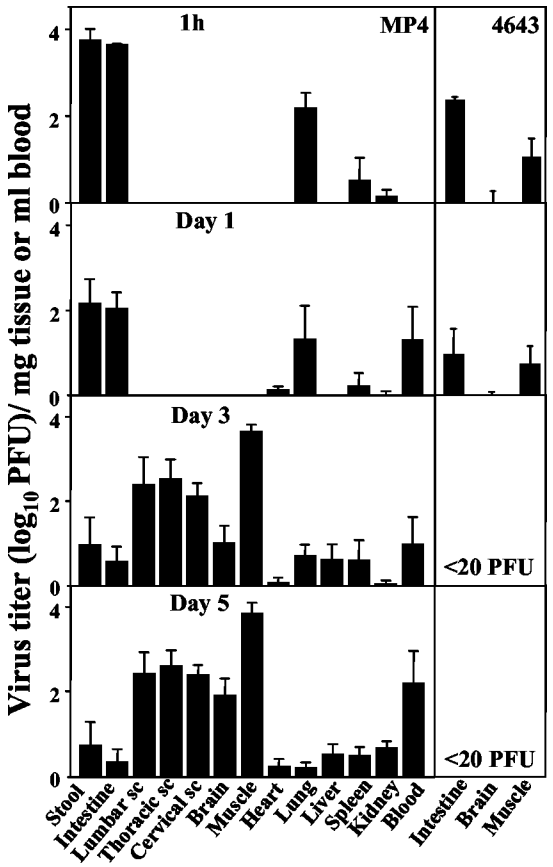

FIG. 7. Tissue viral titers in EV71-infected mice. Seven-day-old mice were inoculated with the parental (Tainan/4643/98) or mouse-adapted (MP4) EV71 strain (5×10^6 PFU/mouse, 200 μl). Viral titers were assessed by plaque assays of tissues collected at the times indicated. Results represent the mean virus titer ($\log_{10}$ PFU) per milligram of tissue or per milliliter of blood ± SEM (six mice per group).

Presence and replication of EV71 in tissues. Virus isolation revealed that MP4 replicated in different organs postinoculation. Specifically, both intestinal tissues and stool samples contained high virus titers ($>10^4$ PFU/mg) at 1 h postinoculation, which decreased gradually thereafter ($<10^2$ PFU/mg at 3 dpi) (Fig. 7). With a low titer (10^1 to 10^2 PFU/ml), viremic spread was detected after 1 dpi. The virus was undetectable in the limb muscle, brain, and spinal cord tissues before 1 dpi, whereas a marked increase (10^2 to 10^4 PFU/mg) was noted at 3 dpi, and the titer remained high until at least 5 dpi. In general, the muscle tissue contained the highest titer (10^4 PFU/mg), which was approximately 1 log higher than those of the spinal cord and brain. In other tissues, including the heart, lung, liver, and kidney, virus titers mostly appeared after 1 dpi and were at least 2 to 3.5 $\log_{10}$ lower than those in the CNS and muscle tissues. Immunohistochemical staining using anti-EV71 VP-1 protein MAb confirmed that the viral protein was present in the CNS (Fig. 6). The cell bodies of neurons (single or in groups) stained strongly. The limb muscle also exhibited strong immunostaining for VP-1 (data not shown). The virus was detected in the intestines of 4643-infected mice ($n = 6$) 1 h postinoculation (2.4 ± 0.1 log PFU/mg). The viral titer was decreased 10-fold at 1 dpi (1.0 ± 1.2 log PFU/mg), and no virus was detected in any tissues thereafter, indicating rapid viral clearance. Immunostaining revealed that virus antigens were present only in the villous epithelia of 4643-infected mice at 1 dpi (data not shown), confirming that the virus did not spread to the CNS after inoculation p.o.

TABLE 2. Nucleotide changes and amino acid substitutions in mouse-adapted EV71 strain MP4[a]

Region	Nucleotide			Amino acid		
	Position	In 4643	In MP4	Position	In 4643	In MP4[b]
VP2	982	C	T			NC
	1093	T	C			NC
	1398	A	T	218	K	L
2C	4385	G	C			NC
	4387	C	T	1214	A	P
	4388	C	A	1215	L	R
	4389	T	G			NC
	4411	C	G			NC
	4414	G	C	1223	M	I
	4431	A	T	1229	H	L
	4985	G	T			NC

[a] Previously determined nucleotide sequences of EV71 strain Tainan/4643/98 have been deposited in GenBank (under accession number AF304458).
[b] NC, no change from the amino acid in 4643.

Sequence comparison of parental and mouse-adapted EV71 strains. To identify whether mutation influences the mouse virulence phenotype, we determined the entire nucleotide and deduced amino acid sequences of the MP4 genome and compared them with those of the parental strain. The two strains share more than 99% nucleotide and amino acid identities, indicating a close genetic relation between these variants. However, there were a total of 15 nucleotide changes in the genome of EV71 strain MP4, including 3 on the VP2 region, 8 on the 2C region, and 4 on the 5′ UTR (Table 2 and Fig. 8). Correspondingly, the deduced amino acid sequences revealed that these nucleotide changes resulted in a 218K-to-L amino acid substitution in the structural VP2 protein and 1214A-to-P, 1215L-to-R, 1223M-to-I, and 1229H-to-L substitutions in the nonstructural 2C protein. The GOR IV program indicated that there was no change in the secondary structure of the VP2 protein. However, the four amino acid substitutions might affect an alpha helix of the 2C protein (amino acids 1208 to 1226) (data not shown). Among the four nucleotide changes on the 5′ UTR (nt40C-to-T, nt307C-to-T, nt498A-to-G, and nt577C-to-T), three of them (at positions 307, 498, and 577) were located within the IRES. Since it has been reported that mutations in the IRES region could confer the enterovirus mouse neurovirulence phenotype (24), we therefore further compared the nucleotide sequences of the 5′ UTRs of three clinical isolates (4643, 6356, and 5746) and MP4. Interestingly, regardless of the virus strain, all of the nucleotide changes clustered at six particular positions (nt 40, 125, 307, 498, 577, and 727) (Fig. 8), suggesting that the 5′ UTR contains mutation hot spots that may be essential for the virulence of EV71.

DISCUSSION

In the present study, we have found that EV71 pathogenicity in mice was increased after mouse adaptation. Strain MP4,

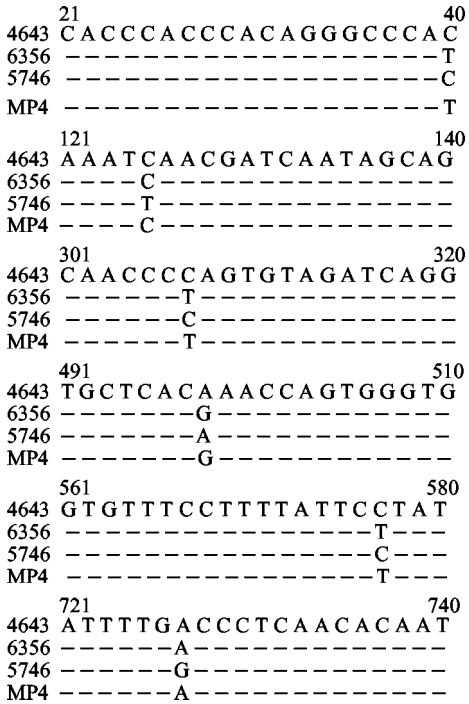

FIG. 8. Alignment of the nucleotide sequences of the 5′ UTRs of EV71 strains reveals six mutation hot spots. The first two isolates, Tainan/4643/98 (GenBank accession number AF304458) and Tainan/6356/98, are associated with encephalomyelitis, and the Tainan/5746/98 (accession number AF304457) strain is associated with HFMD. Only the areas with nucleotide variations are shown.

which was recovered after four serial passages of the parental EV71 strain, 4643, in the brains of mice, showed increased virulence in 1-day-old mice following i.p. inoculation and exhibited rapid growth and a cytotoxic phenotype in vitro. More importantly, intragastric inoculation of strain MP4 in young mice resulted in CNS damage and a disease mimicking some of the features of EV71 infection in humans. Sequence analysis showed that increased virulence of the mouse-adapted viruses is associated with mutations in the VP2 and 2C regions and the 5′ UTR of the MP4 genome.

The parental EV71 strain 4643, an isolate from throat swabs of an 18-month-old patient with encephalitis, has been used in studies of its pathogenesis in mice (31). Inoculation i.p. of strain 4643 caused paralysis and death in 1-day-old mice. However, as demonstrated in this study, strain 4643 was nonpathogenic to 7-day-old mice when it was acquired via oral infection. There was only a transient colonization of the virus in the villous epithelium. In contrast, after oral inoculation, strain MP4 rapidly spread to and replicated in the CNS. It is likely that a mutant(s) develops during the adaptation process, resulting in significant variations in the pathogenesis of MP4 compared to that of the natural virus isolate. However, it is unlikely that the MP4 variant acquires the capacity to recognize a surface molecule of neurons as the virus receptor, since the degree of virulence of 4643 in mice appears to be less than that of MP4 only when delivered via p.o. inoculation. Strain 4643 maintains its neurovirulence, since it was able to induce apoptosis of SK-N-SH cells as MP4 did.

To identify the molecular determinants of the virulence of strain MP4, we sequenced and compared the whole genomes of various EV71 strains. Although both the genome and amino acid sequences of strains MP4 and 4643 show >99% identity, there were nucleotide changes and amino acid substitutions in the VP2 and 2C regions and the 5′ UTR of the MP4 genome. As in other enteroviruses, VP2 has been identified as a part of a deep cleft on the virion surface that may function as the site of virion attachment to a cellular receptor. The 2C protein may have two functions during viral RNA synthesis: as a nucleoside triphosphatase and as director of replication complexes to cell membranes (23). The predicted secondary structure suggested that there was no change in the VP2 protein of the MP4 virus. On the other hand, the amino acid substitutions altered an alpha helix of the 2C protein. It is not known whether this change might contribute to the virulence phenotype of MP4. Interestingly, we detected six hot spots of point mutations in the 5′ UTRs of various EV71 strains. More importantly, strain MP4 is different from 4643 in that it has three nucleotide mutations in the IRES (nt307C-to-T, nt498A-to-G, and nt577C-to-T). We consider that these unique mutations might be responsible for the acquisition of a highly virulent form of EV71, as reported for other enteroviruses. Dunn et al. (5) showed that the 5′ UTR was the primary site considered in the determination of the natural cardiovirulence phenotype of coxsackievirus B3. Ochs et al. (22) showed that a single point mutation in the IRES secondary-structure domain of the poliovirus Sabin vaccine strains is a major determinant of neurovirulence attenuation. This single-nucleotide exchange impairs the interaction of the standard translation initiation factor eIF4G with the domain V. A recent study indicated that EV71 contains a type I IRES (25). We speculate that a mutation(s) in the IRES increases the efficiencies of viral replication processes, which might account for the increase in virulence of EV71 in orally infected mice. In fact, strain MP4 showed a large-plaque phenotype and replicated to a higher level more rapidly than did strain 4643 in vitro, indicating that the MP4 infection cycle is more efficient than that of 4643. Consistently, virus titers in tissue were high in MP4-infected mice, whereas the virus was not detected in 4643-infected mice. Thus, EV71 may utilize the same way to achieve high virulence and neurotropism. It is questionable to link the pathogenicity of EV71 in mice with its pathogenicity in humans. However, the selection of virulence mutants in mice suggests the possibility of a similar selection of mutants that are pathogenic for humans. In addition, we cannot rule out the possibility that strain 4643 is more susceptible to the immune response of the gut.

The neurological manifestation and the CNS lesions of MP4-infected mice reflect the neurotropism and neurovirulence of the virus. Kinetics studies showed that after p.o. inoculation, virus replication was first observed in the intestine. Virus replication was next observed in the limb muscles and spinal cord and then ascending to the brain. Nissl staining revealed that strain MP4 had a restricted tissue tropism in the CNS and that those neurons in the ventral horn regions as well as the brain stem were most vulnerable to EV71. This localization pattern of lesions is dissimilar to those reported in studies on cynomolgus monkeys, which showed that EV71 might have a wider neurotropism than that of polioviruses (20). The limb muscle tissues of MP4-infected mice contained

a vast amount of virus, indicating that the muscle was also a target of EV71 infection and a major site for viral replication in mice. In fact, RD cells were found to be more permissive to EV71 infection than SK-N-SH and Caco-2 cells (approximately 1 log higher after 24 h of incubation [Fig. 1B]). A preliminary study showed that strain MP4 could spread to CNS after intramuscular inoculation (Y. C. Yao and C. K. Yu, unpublished observation), suggesting a retrograde transmission of the virus from peripheral sites to the CNS. Since the disease in EV71-infected mice could be readily attenuated by anti-EV71 Ab, viremia seems to be necessary for the spread of the virus, and neuroinvasion is most likely preceded by virus replication in extraneural tissues.

How MP4 induced mortality is not known. The 2A and 3C protease activities of EV71 have been reported to induce apoptosis of human fibroblasts (11) and glioblastoma cells (12), respectively. We demonstrated that EV71 triggered apoptosis of SK-N-SH cells in vitro and that EV71 infection of mice resulted in apoptosis of neural cells. Concomitantly, CNS tissues had a much higher viral load and displayed more severe tissue damage than other internal tissues. Thus, apoptosis may be involved in the pathogenesis of EV71 infection in mice. The finding that SK-N-SH cells were more susceptible than Caco-2 cells to EV71-induced apoptosis further supported the idea that EV71 was neurotropic. Mononuclear cell infiltration in the CNS was not prominent in EV71-infected mice. It was probably due to the severe depletion of leukocytes after infection. Pulmonary edema has been reported to be frequently associated with fatal EV71 infections in children (8, 18); however, it was not observed in mice with brain stem lesions. Furthermore, the lung as well as the heart tissues of EV71-infected mice contained very little virus. On the other hand, the muscles contained a high viral load and displayed severe necrotizing myositis. Whether the muscle lesions contribute to death is not known. Interestingly, skeletal muscle involvement is seldom reported in the literature concerning EV71 pathogenesis. To our knowledge, this is the first report showing that EV71 displays strong myotropism.

There are some other important observations from this study. First, during active infection, the virus is present in the stools. Transmission of EV71 between infected and noninfected littermates occurred after close contact, as indicated by the occurrence of seroconversion and the presence of viable virus in the stool samples of noninfected littermates. These results support the idea that the common transmission route of EV71 is fecal-oral. Second, disease in EV71-infected mice was readily attenuated by anti-EV71 Ab, indicating that humoral immunity is protective in this model system.

In conclusion, in the studies reported here, we have demonstrated that mouse adaptation could increase the virulence of EV71 in mice. MP4, a mouse-adapted EV71 strain with mutations in the VP2 and 2C regions and the 5′ UTR, showed increased virulence when it was delivered via oral inoculation. This infection model provides a useful tool for vaccine development and therapeutic assessment. Study of the mutations in the mouse-adapted EV71 strain will shed light on the neurovirulence of the virus.

REFERENCES

1. **Alexander, J. P., Jr., L. Baden, M. A. Pallansch, and L. J. Anderson.** 1994. Enterovirus 71 infections and neurologic disease—United States, 1977–1991. J. Infect. Dis. **169:**905–908.
2. **Chan, K. P., K. T. Goh, C. Y. Chong, E. S. Teo, G. Lau, and A. E. Ling.** 2003. Epidemic hand, foot and mouth disease caused by human enterovirus 71, Singapore. Emerg. Infect. Dis. **9:**78–85.
3. **Chen, Y. C., C. K. Yu, Y. F. Wang, C. C. Liu, I. J. Su, and H. Y. Lei.** 2004. A murine oral enterovirus 71 infection model with central nervous system involvement. J. Gen. Virol. **85:**69–77.
4. **Chumakov, M., M. Voroshilova, L. Shindarov, I. Lavrova, L. Gracheva, G. Koroleva, S. Vasilenko, I. Brodvarova, M. Nikolova, S. Gyurova, M. Gacheva, G. Mitov, N. Ninov, E. Tsylka, I. Robinson, M. Frolova, V. Bashkirtsev, L. Martiyanova, and V. Rodin.** 1979. Enterovirus 71 isolated from cases of epidemic poliomyelitis-like disease in Bulgaria. Arch. Virol. **60:**329–340.
5. **Dunn, J. J., N. M. Chapman, S. Tracy, and J. R. Romero.** 2000. Genomic determinants of cardiovirulence in coxsackievirus B3 clinical isolates: localization to the 5′ nontranslated region. J. Virol. **74:**4787–4794.
6. **Gutiérrez, A. L., M. Denova-Ocampo, V. R. Racaniello, and R. M. del Angel.** 1997. Attenuating mutations in the poliovirus 5′ untranslated region alter its interaction with polypyrimidine tract-binding protein. J. Virol. **71:**3826–3833.
7. **Hashimoto, I., and A. Hagiwara.** 1982. Pathogenicity of a poliomyelitis-like disease in monkeys infected orally with enterovirus 71: a model for human infection. Neuropathol. Appl. Neurobiol. **8:**149–156.
8. **Ho, M., E. R. Chen, K. H. Hsu, S. J. Twu, K. T. Chen, S. F. Tsai, J. R. Wang, S. R. Shih, et al.** 1999. An epidemic of enterovirus 71 infection in Taiwan. N. Engl. J. Med. **341:**929–935.
9. **Hsiung, G. D.** 1994. Virus assay, neutralization test and antiviral assay, p. 46–55. *In* G. D. Hsiung, C. K. Y. Fong, and M. L. Landry (ed.), Hsiung's diagnostic virology, 4th ed. Yale University Press, New Haven, Conn.
10. **Huang, C. C., C. C. Liu, Y. C. Chang, C. Y. Chen, S. T. Wang, and T. F. Yeh.** 1999. Neurologic complications in children with enterovirus 71 infection. N. Engl. J. Med. **341:**936–942.
11. **Kuo, R. L., S. H. Kung, Y. Y. Hsu, and W. T. Liu.** 2002. Infection with enterovirus 71 or expression of its 2A protease induces apoptotic cell death. J. Gen. Virol. **83:**1367–1376.
12. **Li, M. L., T. A. Hsu, T. C. Chen, S. C. Chang, J. C. Lee, C. C. Chen, V. Stollar, and S. R. Shih.** 2002. The 3C protease activity of enterovirus 71 induces human neural cell apoptosis. Virology **293:**386–395.
13. **Lin, T. Y., L. Y. Chang, S. H. Hsia, Y. C. Huang, C. H. Chiu, C. Hsueh, S. R. Shih, C. C. Liu, and M. H. Wu.** 2002. The 1998 enterovirus 71 outbreak in Taiwan: pathogenesis and management. Clin. Infect. Dis. **34**(Suppl. 2)**:**S52-S57.
14. **Lin, T. Y., L. Y. Chang, Y. C. Huang, K. H. Hsu, C. H. Chiu, and K. D. Yang.** 2002. Different proinflammatory reactions in fatal and non-fatal enterovirus 71 infections: implications for early recognition and therapy. Acta Paediatr. **91:**632–635.
15. **Lin, T. Y., S. H. Hsia, Y. C. Huang, C. T. Wu, and L. Y. Chang.** 2003. Proinflammatory cytokine reactions in enterovirus 71 infections of the central nervous system. Clin. Infect. Dis. **36:**269–274.
16. **Liu, C. C., H. W. Tseng, S. M. Wang, J. R. Wang, and I. J. Su.** 2000. An outbreak of enterovirus 71 infection in Taiwan, 1998: epidemiologic and clinical manifestations. J. Clin. Virol. **17:**23–30.
17. **Malnou, C. E., T. A. Pöyry, R. J. Jackson, and K. M. Kean.** 2002. Poliovirus internal ribosome entry segment structure alterations that specifically affect function in neuronal cells: molecular genetic analysis. J. Virol. **76:**10617–10626.
18. **McMinn, P. C.** 2002. An overview of the evolution of enterovirus 71 and its clinical and public health significance. FEMS Microbiol. Rev. **26:**91–107.
19. **Minor, P. D.** 1992. The molecular biology of poliovaccines. J. Gen. Virol. **73:**3065–3077.
20. **Nagata, N., H. Shimizu, Y. Ami, Y. Tano, A. Harashima, Y. Suzaki, Y. Sato, T. Miyamura, T. Sata, and T. Iwasaki.** 2002. Pyramidal and extrapyramidal involvement in experimental infection of cynomolgus monkeys with enterovirus 71. J. Med. Virol. **67:**207–216.
21. **Nolan, M. A., M. E. Craig, M. M. Lahra, W. D. Rawlinson, P. C. Prager, G. D. Williams, A. M. Bye, and P. I. Andrews.** 2003. Survival after pulmonary edema due to enterovirus 71 encephalitis. Neurology **60:**1651–1656.
22. **Ochs, K., A. Zeller, L. Saleh, G. Bassili, Y. Song, A. Sonntag, and M. Niepmann.** 2003. Impaired binding of standard initiation factors mediates poliovirus translation attenuation. J. Virol. **77:**115–122.
23. **Racaniello, V. R.** 2001. Picornaviridae: the viruses and their replication, p. 685–722. *In* D. M. Knipe and P. M. Howley (ed.), Fields virology, 4th ed., vol. 1. Lippincott Williams and Wilkins, Philadelphia, Pa.

23a. **Reed, L. J., and H. Muench.** 1938. A simple method of estimating 50 per cent end-points. Am. J. Hyg. **27:**493–497.

24. **Rinehart, J. E., R. M. Gómez, and R. P. Roos.** 1997. Molecular determinants for virulence in coxsackievirus B1 infection. J. Virol. **71:**3986–3991.
25. **Thompson, S. R., and P. Sarnow.** 2003. Enterovirus 71 contains a type I

IRES element that functions when eukaryotic initiation factor eIF4G is cleaved. Virology **315:**259–266.
26. **Tu, Z., N. M. Chapman, G. Hufnagel, S. Tracy, J. R. Romero, W. H. Barry, L. Zhao, K. Currey, and B. Shapiro.** 1995. The cardiovirulent phenotype of coxsackievirus B3 is determined at a single site in the genomic 5′ nontranslated region. J. Virol. **69:**4607–4618.
27. **Wang, S. M., H. Y. Lei, K. J. Huang, J. M. Wu, J. R. Wang, C. K. Yu, I. J. Su, and C. C. Liu.** 2003. Pathogenesis of enterovirus 71 brainstem encephalitis in pediatric patients: roles of cytokines and cellular immune activation in patients with pulmonary edema. J. Infect. Dis. **188:**564–570.
28. **Wang, S. M., C. C. Liu, H. W. Tseng, J. R. Wang, C. C. Huang, Y. J. Chen, Y. J. Yang, S. J. Lin, and T. F. Yeh.** 1999. Clinical spectrum of enterovirus 71 infection in children in southern Taiwan, with an emphasis on neurological complications. Clin. Infect. Dis. **29:**184–190.
29. **Yan, J. J., I. J. Su, P. F. Chen, C. C. Liu, C. K. Yu, and J. R. Wang.** 2001. Complete genome analysis of enterovirus 71 isolated from an outbreak in Taiwan and rapid identification of enterovirus 71 and coxsackievirus A16 by RT-PCR. J. Med. Virol. **65:**331–339.
30. **Yang, K. D., M. Y. Yang, C. C. Li, S. F. Lin, M. C. Chong, C. L. Wang, R. F. Chen, and T. Y. Lin.** 2001. Altered cellular but not humoral reactions in children with complicated enterovirus 71 infections in Taiwan. J. Infect. Dis. **183:**850–856.
31. **Yu, C. K., C. C. Chen, C. L. Chen, J. R. Wang, C. C. Liu, J. J. Yan, and I. J. Su.** 2000. Neutralizing antibody provided protection against enterovirus type 71 lethal challenge in neonatal mice. J. Biomed. Sci. **7:**523–528.
32. **Zheng, Z. M., P. J. He, D. Caueffield, M. Neumann, S. Specter, C. C. Baker, and M. J. Bankowski.** 1995. Enterovirus 71 isolated from China is serologically similar to the prototype E71 BrCr strain but differs in the 5′-noncoding region. J. Med. Virol. **47:**161–167.